

Semi-supervised identification of SARS-CoV-2 molecular targets

Kristen L. Beck,^{1*} Ed Seabolt,^{1*} Akshay Agarwal,¹ Gowri Nayar,¹ Simone Bianco,^{1,2}
Harsha Krishnareddy,¹ Vandana Mukherjee,¹ James H. Kaufman¹

¹AI and Cognitive Software, IBM Almaden Research Center, San Jose, CA USA

²NSF Center for Cellular Construction, San Francisco, CA USA

*To whom correspondence should be addressed:

klbeck@us.ibm.com, eseabolt@us.ibm.com

SARS-CoV-2 genomic sequencing efforts have scaled dramatically to address the current global pandemic and aid public health. In this work, we analyzed a corpus of 66,000 SARS-CoV-2 genome sequences. We developed a novel semi-supervised pipeline for automated gene, protein, and functional domain annotation of SARS-CoV-2 genomes that differentiates itself by not relying on use of a single reference genome and by overcoming atypical genome traits. Using this method, we identified the comprehensive set of known proteins with 98.5% set membership accuracy and 99.1% accuracy in length prediction compared to proteome references including Replicase polyprotein 1ab (with its transcriptional slippage site). Compared to other published tools such as Prokka (base) and VAPiD, we yielded an 6.4- and 1.8-fold increase in protein annotations. Our method generated 13,000,000 molecular target sequences— some conserved across time and geography while others represent emerging variants. We observed 3,362 non-redundant sequences per protein on average within

18 **this corpus and describe key D614G and N501Y variants spatiotemporally.**
19 **For spike glycoprotein domains, we achieved greater than 97.9% sequence**
20 **identity to references and characterized Receptor Binding Domain variants.**
21 **Here, we comprehensively present the molecular targets to refine biomedical**
22 **interventions for SARS-CoV-2 with a scalable high-accuracy method to ana-**
23 **lyze newly sequenced infections.**

24 **1 Introduction**

25 The ongoing SARS-CoV-2 pandemic has undoubtedly shaped our lives as one of the most
26 significant global health challenges we are facing. However, unlike previous pandemics, we
27 now have sequencing technology with tremendous throughput to analyze the genomic content
28 of SARS-CoV-2. As labs around the world sequence isolates from infected individuals, we
29 can track and characterize the viral genome evolution in almost near real-time as the pandemic
30 keeps infecting the worldwide population.

31 The first sequenced SARS-CoV-2 genome (*I*) was submitted to NCBI January 17, 2020
32 and has become the accepted reference standard commonly referred to as the Wuhan reference
33 genome (NCBI RefSeq ID: NC_045512.2). Since that point, tens of thousands of genomes are
34 published on a weekly basis. The SARS-CoV-2 genome is comprised of a 29,000 base pairs (bp)
35 single-stranded RNA (38% GC content) with four structural proteins, two large polyproteins
36 which are cleaved to form non-structural proteins, and several accessory proteins (2, 3). There
37 are two overlapping open reading frames responsible for Replicase polyprotein 1a (pp1a) and
38 Replicase polyprotein 1ab (pp1ab) which yield the longest products from the genome and the
39 majority of the non-structural proteins.

40 In comparison to other coronaviruses, SARS-CoV-2 differs phenotypically with its signif-
41 icant increase in transmissibility and asymptomatic or presymptomatic transmission, as well

42 as genotypically from its polybasic cleavage site insertion in the S protein (4). However, it
43 maintains several other *Coronaviridae* traits such as gene order consistency and transcriptional
44 slippage (5). The -1 programmed ribosomal frameshift responsible for transcriptional slippage
45 has been observed to occur at the point where ORF1 (responsible for pp1a) continues as ORF2
46 (responsible for pp1ab) and is defined by an RNA signature marking the slippery site (6). This
47 phenomenon allows the virus to control the relative levels of its protein expression (6) and may
48 be useful in therapeutic targeting to limit protein production. Additionally, this unique trait
49 creates a challenge for traditional bioinformatic genome annotation programs which assume
50 that the more typical continuous 5' to 3' translation can be effectively used to form the correct
51 protein sequence which is not the case for SARS-CoV-2.

52 There are several viral genome annotation methods such as VAPiD, Prokka, InterProScan,
53 and others (7–9) that aim to provide autonomous (that is, no reference genome required) annota-
54 tion of genes and proteins. Some of these tools have issued special releases to aid in annotating
55 SARS-CoV-2 genomes. Yet, many of these tools do not provide sufficient accuracy with “off
56 the shelf” use and have not yet been applied at scale as the available SARS-CoV-2 sequence
57 data grows. Additionally, several variants of SARS-CoV-2 genomes have emerged including the
58 D614G (10) variant, which appeared earlier in the pandemic, or the more recent B.1.1.7 vari-
59 ant (11, 12), which now represents the majority of new cases in the USA (13). The mutations
60 defining these variants can present challenges for complete automation of genome annotation
61 and this can be further exacerbated by the SARS-CoV-2 transcriptional slippage site.

62 As an alternative to an autonomous genome annotation method, alignments to the Wuhan
63 reference genome (1) using tools such as NextStrain’s Augur (14), Bowtie2 (15), or UCSC
64 SARS-CoV-2 genome browser (3) can be completed. This type of supervised analysis uses
65 published gene coordinates to extract sequences from the query genome based on positional
66 and sequence similarity to a reference genome. However, this creates a considerable depen-

67 dency on a single reference genome. Since it is currently estimated that SARS-CoV-2 typically
68 mutates approximately twice per month on any given transmission chain (*16*) and can be sub-
69 ject to recombination events (*17*), a reference-guided approach may face limitations as the virus
70 continues to evolve or increases the rate at which it evolves.

71 In this work, we present a semi-supervised custom pipeline to annotate all genes, proteins,
72 and functional domains for SARS-CoV-2. This method has been applied to 66,905 SARS-
73 CoV-2 genomes collected from NCBI GenBank (*18*) and GISAID (*19*). This approach yielded
74 nearly 13 million new molecular sequences and connections that can be accessed through the
75 IBM Functional Genomics Platform, a tool made freely available to the global research commu-
76 nity (*20*). With our method, we achieved 98.5% average protein set membership identification
77 accuracy and an average observed over expected protein length ratio of 99.1%. Additionally,
78 in comparison to other tools such as Prokka or VAPiD, we identified 6.4- and 1.8-fold more
79 protein annotations, respectively. Furthermore in a targeted analysis, we achieved greater than
80 97.9% sequence identity in spike glycoprotein domains.

81 To illustrate the value of this approach, we utilized the variants identified in this collection
82 to track the emergence of the D614G and N501Y spike glycoprotein variants over time and by
83 region of exposure. The complete collection of SARS-CoV-2 genes, proteins, and functional
84 domains continues to be updated and can be accessed via a web browser user interface or our
85 developer toolkit.¹ Ultimately, we present a comprehensive comparative analysis and data re-
86 source of 66,905 publicly available SARS-CoV-2 viral sequences, with the aim of identifying
87 potential targets to aid in vaccine, diagnostic, or therapeutic development.

¹<https://ibm.biz/functional-genomics>

88 **2 Results**

89 Here, we present a novel semi-supervised pipeline to annotate gene, protein, and functional
90 domain molecular targets from SARS-CoV-2 genomes and demonstrate the resulting accuracy
91 against known reference data and other bioinformatic tools (see Methods). This pipeline pro-
92 vides improvements over base Prokka and InterProScan by adding a novel capability that more
93 accurately processes sequences the slippery site junction in Replicase polyprotein 1ab to iden-
94 tify the correct sequence which is absent or artificially truncated in other methods. Additionally,
95 we incorporated a targeted search for three key proteins: ORF9b, ORF10, and Envelope small
96 membrane protein which would otherwise be missing in the protein annotation set. We show
97 that our pipeline has an improvement on annotation accuracy by 1.8- and 6.4-fold compared to
98 VAPiD and base Prokka. We also evaluated genome quality from data in public repositories
99 and quantitatively evaluated commonly used quality criteria for their effects on the resulting
100 annotations.

101 **2.1 Assessment of SARS-CoV-2 genome quality in multiple data sources**

102 For effective genome annotation, an important first step is to assess the quality of the input
103 genomes. In this study, we analyzed a corpus of 66,905 SARS-CoV-2 genomes (Supplemen-
104 tary File 1) deposited over the span of eight months from 108 countries into two key aggregate
105 data sources: GISAID (19) and NCBI GenBank (18). We observed an average of 0.0067%
106 unknown bases (denoted as N per IUPAC definitions) per genome (range 0–46.76%), and all
107 genomes were observed to have less than 1% degenerate bases (Figure 1a). The presence of
108 unknown bases can indicate insufficient genome coverage or other issues from genome assem-
109 bly. Next, we aimed to identify criteria for inclusion of a SARS-CoV-2 genome assembly into
110 our platform to ensure that input data for molecular target identification is of the highest quality.
111 Therefore, we evaluated two commonly used criteria for their effects on prediction of full length

112 protein sequences. Briefly, Criteria A is more permissive and prioritizes the ratio of length vs.
113 coverage whereas Criteria B is more stringent and applies a higher penalty to the number of gaps
114 (detailed definitions in Section 4.1). Here, “full length” is defined as a protein sequence length
115 within 10% of the known UniProt protein reference sequence indicated in the SARS-CoV-2
116 proteome as defined in ViralZone (21, 22). Figure 1b demonstrates that Criteria A yielded the
117 highest count of full length protein products (35,099 non-redundant protein sequences) while
118 also effectively reducing the majority of truncated products (2,197 non-redundant protein se-
119 quences). If applying the more stringent Criteria B, over 14,000 high quality protein products
120 would be inadvertently removed. Based on this, we proceeded with applying the thresholds
121 defined by Criteria A to the corpus of genomes analyzed in this work. From GISAID and
122 GenBank genomes, 9.9% (out of 55,708) and 3.1% (out of 11,197) of genomes fell below this
123 criteria (Figure 1a) and are removed from subsequent analysis and marked as inactive unless
124 otherwise mentioned.

125 As part of our other pre-processing steps for genomic data (20), we computed md5 hashes
126 of all genome sequences to track duplicates. The rate of ‘duplicated’ SARS-CoV-2 genome
127 sequences within a single data source or between data sources is indicated in Table 1. From
128 the data at hand, it is unclear whether these duplicated genome sequences as others have ob-
129 served (23–25) are artefacts of data processing e.g. due to alignments to a single reference
130 genome or are a result of sampling multiple patient infections within the same lineage. Of the
131 10,528 genomes that are duplicated within GISAID, we compared the metadata for each entry:
132 3,953 are described with matching metadata entries in addition to identical full length genome
133 sequences and therefore may be more likely to be data duplication artefacts. These potential
134 duplication events are reported here but are not removed from subsequent analysis.

Source 1	Source 2	Genome Sequence Hashes	Genome Accessions
GISAID	NA	47,908	55,708
GENBANK	NA	9,398	11,196
REFSEQ	NA	1	1
GISAID	GISAID	2,791	10,528
GISAID	GENBANK	5,559	13,977
GENBANK	GENBANK	706	2,504
GISAID	REFSEQ	1	43
GENBANK	REFSEQ	1	11

Table 1: Distribution of Duplicated Genome Sequences. The number of unique genome sequences (count of non-redundant md5 hashes) and total genome accessions (count of all entries) are listed for each source: GISAID, GenBank, and NCBI RefSeq. Then pairwise comparisons are made for each genome sequence to indicate how many times a genome sequence is duplicated (exact md5 match of genome sequence) within its source or between sources and for how many entries this accounts for (count of genome accessions). For RefSeq comparisons, note only one SARS-CoV-2 reference genome sequence is available NC_045512.2

2.2 Quantification of protein sequence prediction accuracy

For an autonomous COVID-19 genome annotation pipeline to achieve clinical and biological relevance, it must accurately identify all known molecular targets within a genome. The SARS-CoV-2 proteome (2,22) is defined as having fourteen protein products each with a corresponding gene sequence present in each genome. SARS-CoV-2 proteins are split into structural and non-structural, but all proteins are required for the virus to carry out its life cycle which includes host cell invasion, replication, and transmission (26). Using our gene and protein annotation method (Section 4.2), we achieved an average per protein identification accuracy of $98.5\% \pm 2.9\%$ across all genomes above the aforementioned quality thresholds. The number of observations per protein (Figure 2a) indicates that we are able to achieve complete or near-complete protein set membership for all genomes. Each protein is a translated gene sequence, and thus the equivalent gene identification accuracy is also achieved.

Furthermore, not only must the complete set of named genes and proteins be identified for accurate genome annotation, but the generated sequences must also be grounded in biological

149 reality. Specifically, *in silico* predicted sequences should not be truncated with respect to the
150 length of known references, and the mutational density must be low considering the temporally
151 recent emergence of SARS-CoV-2 and observed lower mutation rate compared to other RNA
152 viruses (16). Using our semi-supervised gene and protein annotation method (Section 4.2), we
153 were able to identify full length protein products that on a per protein basis match expected
154 lengths of known reference sequences with an average observed / expected protein length value
155 of 99.1% (Figure 2b). The distributions of our predicted and the expected protein sequence
156 lengths are observed to be statistically similar by two-sample Kolmogorov–Smirnov test ($D =$
157 0.0071 , $p < 2.2e-16$) and are 8.75-fold more similar ($D = 0.0617$) than those predicted from
158 genomes not passing our quality thresholds, i.e., inactive genomes.

159 In addition, certain gene and protein sequences required us to develop additional targeted
160 methodological advances for identification (Section 4.2.2). Specifically, Replicase polypro-
161 tein 1ab (pp1ab) is the longest gene sequence within SARS-CoV-2 and its protein sequence is
162 cleaved into 16 non-structural proteins (2). It overlaps with Replicase polyprotein 1a, and dur-
163 ing translation, undergoes -1 programmed ribosomal frame shift at what is known as a slippery
164 site (6). Both of these attributes make it more challenging to accurately identify with off-
165 the-shelf *in silico* genome annotation methods. Therefore, we implemented a semi-supervised
166 method (Section 4.2.2) to correct and extend the putative predicted gene coordinates for pp1ab
167 and adjust the translation method to accommodate ribosomal frame shift which is a problem that
168 negatively affects other bioinformatic tools. Our algorithmic improvement yielded full length
169 pp1ab sequences in all genomes with greater than 95% sequence identity to the reference pp1ab
170 sequence (UniProt ID: P0DTD1) in over 99.15% of the variants we predict (Figure 3).

171 Ultimately from this genome corpus, we were able to identify over 13M gene, protein,
172 and functional domain sequences in total (Table 2). Our system only stores each uniquely
173 identified sequence once (distinct sequence), but maintains the relationship to its originating

174 genome and to any connected sequences e.g. gene, protein, or domain sequence providing the
175 total sequences identified (Table 2).

Type	Total Count	Unique Count
Gene	936,603	59,531
Protein	815,878	42,611
Domain	11,621,784	59,271

Table 2: Observed gene, protein, and functional domain biological entities in total count (redundant) and unique sequences (distinct) in active genomes.

176 **2.3 Comparative analysis of genome annotation methods**

177 With regard to pipeline accuracy, we benchmarked our pipeline against VAPiD (7), which has
178 created a special release for annotating SARS-CoV-2 genomic data, and Prokka (8), a prokary-
179 otic genome annotation tool for bacteria and virus. From the same set of genomes, we con-
180 trasted the resulting protein annotations (Figure 4) in the context of set membership as well as
181 in observed protein sequence length compared to reference protein sequence length (expected).
182 VAPiD and our method both achieved high accuracy with regard to truncated proteins, but our
183 pipeline elicited more proteins in the highest accuracy category and 1.8-fold more protein anno-
184 tations overall (Figure 4). Prokka, on the other hand, did not yield any full length pp1ab protein
185 sequences and generated a high amount of missing or truncated proteins (Figure 4). Our method
186 was able to identify 6.4-fold more protein products compared to base Prokka and was able to
187 generate full-length pp1ab products with high sequence identity to known UniProt references.

188 **2.4 Quantification of domain sequence prediction accuracy**

189 To evaluate functional domain annotation accuracy, we analyzed functional domains for spike
190 glycoprotein (S protein) as this is one of the most studied proteins in SARS-CoV-2 and it is of
191 high biomedical importance. Specifically, we analyzed the set membership completeness of our

192 predicted domains against the domain architecture indicated by InterProScan for the UniProt
193 RefSeq P0DTC2 (<https://www.ebi.ac.uk/interpro/protein/reviewed/P0DTC2/>).
194 From 5,702 distinct spike protein sequences, our annotation method yielded an average 94.4%
195 \pm 4.4% domain set membership accuracy (Figure 5a) with only two unexpected domain anno-
196 tations (IPR043002 and IPR043614) found in less than 0.1% of the proteins. For IPR043473,
197 the domain architecture is split across two locations which accurately accounts for the num-
198 ber of observations of this domain being greater than the number of spike proteins analyzed.
199 The corresponding count of distinct sequences for each domain is indicated in Figure 5a and
200 these domains were observed to have 679 unique sequences on average. The S1-subunit of
201 the N-terminal domain for SARS-CoV (IPR044341) and Betacoronaviruses (IPR032500) were
202 observed to have the highest count of non-synonymous variants. Furthermore, we calculated
203 the amino acid percent identity of each of our predicted domain sequences against domain se-
204 quences extracted reference S protein, and all domains achieved greater than 98% median per-
205 cent identity (Figure 5b). Together, this indicates completeness of annotation and correctness
206 of the predicted domain sequences.

207 **2.5 Distributions of variants shift over time**

208 We identified the exhaustive set of genes, proteins, and functional domains (Table 2) for the
209 corpus of genomes indicated previously. The number of variants (distinct sequences) differs per
210 molecular target across all bio-entities as well each variants' frequency (cumulatively shown in
211 the redundant count). As SARS-CoV-2 undergoes mutation events, a comprehensive catalog of
212 variants is essential for developing molecular interventions with sufficient specificity and bind-
213 ing efficiency. We observe a median of 425 unique sequences with non-synonymous mutational
214 differences per protein (the number of unique sequences range=109–19,406) per protein. The
215 S protein which is involved in invasion of human cells through interaction with ACE2 (27) is

216 observed to have the highest number of variants among structural SARS-CoV-2 proteins (Fig-
217 ure 2a). Not surprisingly, the non-structural products of ORF1a and ORF1ab are also observed
218 to have a higher amount of sequence variants compared to other SARS-CoV-2 proteins (Figure
219 2a).

220 Since the S protein is the key gatekeeper of host cell invasion and the target of multiple
221 vaccines, antivirals, and diagnostics, we further examined its observed variants. We observed
222 two predominant S protein variants that shift in their cumulative frequency over time (Figure
223 6a). Initially, an exact match to the reference spike glycoprotein sequence (green line, UniProt:
224 P0DTC2) is observed most frequently. Then in mid-April, the notable variant D614G (orange
225 line) with now known increased infectivity due to interaction with ACE2 receptor (28, 29) over-
226 takes the ancestral reference sequence (green line) in its abundance achieving fixation. Two
227 other differing sequences are observed at lower abundance in this genome cohort and corre-
228 spond to P1140X (olive line) and S2 cleavage product (pink line). Additionally, there are minor
229 variants observed in less than 1% of sequenced genomes. For example, we observe 5 protein se-
230 quences to contain the N501Y mutation from 13 genomes originating from Oceania (submitted
231 2020-07-02) and North America (submitted 2020-06-01). These variants are also observed to
232 contain the D614G mutation, but are not present with the 69-70 deletion present in the B.1.1.7
233 variant of concern (UK) or B.1.351 E484K mutation (South Africa). Our observations are con-
234 sistent with the current understanding of multiple introduction events causing the emergence
235 of the N501Y variant (30). Furthermore, since this variant is observed in the B.1 and B.1.1
236 lineages which predate the current B.1.1.7 and B.1.351 variants it further clarifies the current
237 timing of mutational introduction points in the pandemic. Some of our observed sequence vari-
238 ants may be due sampling to limitations or data artefacts e.g. sequencing or genome assembly
239 error, but if a minor variant confers a selective advantage, its frequency could shift to become
240 a more common variant as we have seen in recent months with the B.1.1.7, P.1, and B.1.351

241 variants (31).

242 When S protein variants are stratified by region of exposure (Figure 6b), the ancestral vari-
243 ant (`uid_key:15060367c74a24be49e99859f5d88544`) is the most predominant pro-
244 portion globally across the corpus (0.42 – 0.80 of observed variants for a given exposure region)
245 whereas the D614G variant (`uid_key:4c35f09aac2f7be4f3cffd30c6aecac8`) is ob-
246 served as a lower proportion per region (range 0.08 – 0.44) the next most prevalent variant. Both
247 of these variants are observed across all exposure regions. Together, these results provide tem-
248 poral and geographic insights about the dominant variants in the population of genomes that
249 have been analyzed in this work. Additionally, our pipeline correctly identifies key D614G and
250 N501Y variants that are been previously observed and experimentally validated (28) further
251 indicating its accuracy.

252 **3 Discussion**

253 Since the start of the SARS-CoV-2 global pandemic, there have been immense efforts globally
254 to sequence with near real-time efficiency the viral genomes observed in infected patients. In
255 order to capitalize on this large and growing corpus of data, high throughput computational
256 methods must be developed for rapid, high accuracy analysis to deliver the molecular targets
257 that are actually under evaluation for drug development, vaccine specificity, and diagnostic
258 testing. The method described here provides one such avenue to accomplish this goal. The
259 protein and domain data generated as part of this work provides these molecular targets in
260 an efficient manner with very high accuracy across the entire SARS-CoV-2 proteome and for
261 all genomes analyzed in this corpus spanning multiple countries and lineages. Beyond this,
262 our semi-supervised pipeline does not require the use of a single reference genome which better
263 allows the detection of novel or mutating gene, protein, and respective domain sequences as they
264 emerge. The method described here has been integrated with our Functional Genomics Platform

265 and applied to hundreds of thousands of SARS-CoV-2 genomes. As the vaccination rates rise
266 and the pandemic continues, this method can be used to rapidly monitor and track emerging
267 protein variants to inform vaccine specificity and host protein binding affinity. Additionally as
268 future work, further confirming the *in silico* predicted sequences using a structural model will
269 allow for refinement of the protein sequences and key domains to expand our understanding
270 of interaction with host proteins, antivirals, or diagnostics. Overall, the data generated as part
271 of this work provides a comprehensive set of protein and domain variants observed globally
272 and supports the research community as we aim to understand and control the SARS-CoV-2
273 pandemic.

274 **4 Methods**

275 We used a combination of state of the art tools and custom calibration tools to provide a semi-
276 supervised genome annotation pipeline. We verified accuracy of, and applied this method to
277 66,905 SARS-CoV-2 genomes to identify the gene, protein, and functional domain sequences
278 contained within each genome. This collection was analyzed for accuracy and quality with
279 regard to current known references. Protein variants are characterized as a function of time
280 since the pandemic emerged and from a geographic perspective.

281 **4.1 Genome Data Retrieval and Quality Thresholds**

282 SARS-CoV-2 genomes were retrieved from the Global Initiative for Sharing All Influenza Data
283 (GISAID) (19) and NCBI GenBank (18) (retrieved August 18, 2020). A complete list of data
284 sources, genome accessions, and acknowledgement of the submitting lab/author information
285 where available is included in Supplemental File 1. An md5 hash was computed on each
286 genome sequence (excluding headers) to track identical genome sequences. In preparation of
287 genome annotation, two commonly used genome quality criteria and thresholds were assessed

288 for their ability to yield a complete set of full length protein sequence annotations. Criteria A
289 is defined as genome length $> 29,000$ bp (only IUPAC characters allowed, gaps permitted), %
290 unknown bases (Ns) < 1 , “high coverage” flag indicated by GISAID defined as $< 0.05\%$ muta-
291 tion density only in CDS, and no unverified indels in relation to all other genomes in GISAID.
292 Criteria B is defined as: number of unknown bases ≤ 15 , number of degenerate bases ≤ 50 ,
293 number of gaps ≤ 2 , and mutation density < 0.25 . For benchmarking genome quality criteria,
294 all genomes were processed with our genome annotation pipeline and their resulting protein se-
295 quences were evaluated. Protein length distributions as a function of this genome criteria were
296 compared using a two-sample Kolmogorov-Smirnov (ks.test function in base R).

297 **4.2 Gene and Protein Annotation**

298 Specific modifications to our previously described genome annotation pipeline (20) were made
299 to process SARS-CoV-2 genomes and yield gene, protein, and domain sequences. In the sub-
300 sections below we describe, in detail, the key modifications of Prokka v1.14.5 (8) for improved
301 unsupervised annotation of SARS-CoV-2 genomes (Section 4.2.1) and the addition of custom-
302 built supervised algorithms to improve identification of specific proteins that were unable to be
303 detected using the base implementation (Section 4.2.2). The method has been Dockerized and is
304 available for use at [https://github.com/IBM/omxware-getting-started/tree/](https://github.com/IBM/omxware-getting-started/tree/master/SARS-CoV-2_parser)
305 [master/SARS-CoV-2_parser](https://github.com/IBM/omxware-getting-started/tree/master/SARS-CoV-2_parser).

306 **4.2.1 Modifications to accommodate SARS-CoV-2 genome attributes and nascent state** 307 **of reference data**

308 To yield gene and protein names, Prokka (8) requires a reference protein database as a BLAST
309 (32) index. We constructed this from the UniProt COVID-19 pre-release reference ([ftp://](ftp://ftp.uniprot.org/pub/databases/uniprot/pre_release/covid-19.dat)
310 [ftp.uniprot.org/pub/databases/uniprot/pre_release/covid-19.dat](ftp://ftp.uniprot.org/pub/databases/uniprot/pre_release/covid-19.dat)).
311 During the build phase for this index (Prokka script: `prokka-uniprot_to_fasta_db`), the

312 following modifications were made and applied during SARS-CoV-2 annotation:

313 1. Modify minimum evidence level required from transcript level (evidence=2) to predicted
314 (evidence=4) when selecting reference proteins. This change allows proteins with evi-
315 dence levels: at the protein level (evidence=1), at the transcript level (evidence=2), in-
316 ferred from homology (evidence=3), or predicted (evidence=4) to be used when building
317 references (but does not include protein uncertain, evidence=5). This is to better accom-
318 modate the nascent state of SAR-CoV-2 protein references.

319 2. Do not assign “hypothetical protein” to recommended full names that start with the fol-
320 lowing regular expression:

321 `/^UPD\d|^Uncharacterized protein|^ORF|^Protein /`

322 as some valid SARS-CoV-2 proteins contain these prefixes e.g. ORF3a protein and Un-
323 characterized protein 14.

324 3. Accept proteins without a recommended full name as long as the entry includes a full
325 name provided by the submitter e.g. ORF10.

326 Based on the above, the BLAST index was built using `prokka-uniprot_to_fasta_db`
327 with the following command parameters: `--verbose --term Viruses --evidence`

328 4. The output of this command was then copied to the
329 `db/kingdom/Viruses` folder of the Prokka distribution to use as reference data.

330 Additionally, if a genome is less than 100,000 bp in length, by default Prokka will auto-
331 matically switch to “metagenome mode” even in the absence of the metagenome flag opposed
332 to persisting in “single genome mode.” To ensure single genomes of SARS-CoV-2 which are
333 29,000 bp were processed appropriately, we added an option named `mintotalbp` to the main

334 `prokka` script which parameterized the minimum total base pairs required before this auto-
335 switch could be activated. We set the default value for `mintotalbp` to 100 bp to avoid this
336 inadvertent mode switch.

337 **4.2.2 Modifications to improve complete and accurate protein identification**

338 Custom processing was developed for ORF9b, ORF10, Envelope small membrane protein, and
339 Replicase polyprotein 1ab. To support additional identification of these sequences, all raw po-
340 tential gene sequence coordinates and their scores were output from Prodigal using `-s` (opposed
341 to only gene coordinates above Prodigal's default threshold) during an intermediate step prior
342 to Prokka with additional modifications as indicated below.

343 For the ORF9b, ORF10, and Envelope small membrane protein, an additional extraction
344 process was completed by parsing that extended potential gene coordinate information. A
345 length search was completed from these putative coordinates where accepted sequences must
346 be within 10% of the reference protein sequence length and be the closest match to known ref-
347 erence sequences within those length bounds. Global alignments between the candidate protein
348 sequence and known references (UniProt IDs: P0DTD2, A0A663DJA2, and P0DTC4 respec-
349 tively) were completed using `pairwise2` in BioPython with BLOSUM62 scoring matrix (33),
350 gap open penalty = -2, and gap extend penalty = -1 to indicate sequence similarity between
351 predicted and known reference sequences.

352 For Replicase polyprotein 1ab (`pp1ab`) important modifications were added beyond this to
353 ensure identification of the full length sequence and to accommodate the naturally occurring
354 -1 programmed ribosomal frameshift (6). We used the raw predicted gene coordinates from
355 Prodigal to extract a candidate gene sequence from the originating genome. However, these
356 candidate coordinates do not yield the full gene length or correct full length `pp1ab` sequence
357 and were therefore modified as follows:

- 358 1. If Prodigal outputs two separate segments of the full gene sequence, we augmented and
359 filled in the missing gap section from the originating genome based on the overall start
360 and end coordinates to yield one contiguous gene sequence.
- 361 2. If Prodigal output only one truncated segment of the full pp1ab gene sequence, we shifted
362 the starting index to ensure that the full length sequence achieved the expected entire
363 21,289 bp known to be part of the reference sequence (UniProt ID:P0DTD1).
- 364 3. In both cases, we verified that the gene sequence begins with an expected start codon
365 (Methionine, ATG) and ends with a proper stop codon (TAA). When identifying the start
366 codon, we verified the expected first three nucleotides were in the predicted sequence and
367 shifted the start index to ensure this was the start position if that was not the case. Then,
368 if the sequence did not include the start codon, we subtracted 1 from the start index until
369 the correct start codon (ATG) was the first three nucleotides. The same procedure was
370 used to ensure that the sequence ended with a proper stop codon, as we add 1 to the end
371 index until TAA were the last three nucleotides.
- 372 4. Next, the slippery site as identified by Kelly, et al. (6) was identified in the gene sequence
373 allowing for nucleotide degeneracy as indicated.
- 374 5. At the point of the slippery site, the preceding base was repeated and the remaining gene
375 sequence was appended to yield the gene sequence which was then translated to yield the
376 full length pp1ab protein sequence.

377 This method for generating complete Replicase polyprotein 1ab sequences was applied to
378 all genomes. Of the 5,055 genomes below our quality control thresholds (inactive genomes),
379 only 3,056 genomes were observed to contain a slippery site and therefore only those were able
380 to be analyzed using this method.

381 **4.3 Protein domain annotation**

382 Unique protein sequences were processed with InterProScan v5.48-83 (9) to identify domain
383 sequences and InterPro (IPR) codes as previously described (20). This version of InterProScan
384 contains a number of InterPro, Gene Ontology and Pathway codes specific to the SARS-CoV-
385 2 proteome and reference data. A full list of all available codes can be found at <https://www.ebi.ac.uk/interpro/proteome/uniprot/UP000464024/>.

387 **4.4 Comparative analysis**

388 To compare our method against other published viral genome annotation tools, VAPiD (v1.2
389 with Python3) was run on a set of 100 randomly selected SARS-CoV-2 genomes above quality
390 control thresholds previously defined in Section 4.1 using the following parameters: reference
391 (`--r`) NC_045512.2. Protein names and sequences were extracted from VAPiD output files
392 using BioPython's parser. Prokka version 1.14.5 (8) was run on this same set of genomes using
393 default parameters with `--kingdom` Viruses. The resulting protein sequences from each
394 tool were compared for set membership per genome, protein sequence truncations, and overall
395 sequence similarity.

396 Protein annotations were evaluated against the SARS-CoV-2 proteome reference sequences
397 indicated in ViralZone, SIB Swiss Institute of Bioinformatics (22) for complete protein set
398 membership per genome, sequence length, and sequence similarity to known references indi-
399 cated in NCBI UniProt (21). Set membership accuracy is the count of observations of a given
400 protein for a set of genomes analyzed or in the case of domains, the set of domain sequences
401 annotated for a given protein.

402 For domain accuracy comparative analysis, our predicted domains identified in spike glyco-
403 protein (S protein) were analyzed for set membership completeness against the expected Inter-
404 Pro domain architecture for UniProt reference sequence P0DTC2 (<https://www.ebi.ac>.

uk/interpro/protein/reviewed/P0DTC2/). Additionally, where predicted domain sequences were assigned an IPR code (8,146 unique domain sequences out of 9,120 total domain sequences), the predicted domain sequence was compared against the reference sequence to yield a percent identity. Reference domain sequences were extracted from the S protein amino acid sequence (UniProt:P0DTC2) based on domain start and stop sites indicated at the link above. Amino acid percent identity was calculated with considerations for insertions, deletions, or substitutions.

For genome to genome and protein variant comparisons (Sections 2.1 and 2.5), genome-associated metadata was retrieved from GISAID and processed for each analysis. For duplicated genome identification, an md5 of the genome sequence (excluding header) was completed as described in 4.1. Originating lab, date submitted, and host fields were used to further characterize candidate duplicate genome sequences. For protein variant analysis, the date submitted and exposure region fields are used to describe the time and geography of the observed variants.

4.5 Data Availability

The Functional Genomics Platform is available at <https://ibm.biz/functional-genomics>. Access to the data generated from the method described herein is available through a developer toolkit (REST services, omxware Python SDK, and Docker container) or web interface, which can be accessed by requesting credentials at the link above. This includes the data described in this manuscript as well as the continual update of new identifications. Additionally pertaining to this manuscript, protein and domain sequence data are provided in Supplemental Files 2 and 4, respectively with identifier mappings described in Supplemental Files 3 and 5. All the GISAID data is available at www.gisaid.org.

428 **5 Author Contributions**

429 KLB, ES, and VM conceived of this work. KLB, ES, GN, and AA designed the experiments.
430 KLB, ES, GN, AA, and HK generated and analyzed the data. KLB, ES, GN, and AA wrote
431 the manuscript. SB, VM, JK analyzed the data and oversaw the experiments. All co-authors
432 revised and approved the manuscript.

433 **6 Competing Interests**

434 The authors declare no competing interests.

435 **References**

- 436 1. Wu, F. *et al.* A new coronavirus associated with human respiratory disease in China. *Nature*
437 **579**, 265–269 (2020). URL <https://pubmed.ncbi.nlm.nih.gov/32015508/>.
- 438 2. Yoshimoto, F. K. The Proteins of Severe Acute Respiratory Syndrome Coronavirus-2
439 (SARS CoV-2 or n-COV19), the Cause of COVID-19 (2020). URL <https://doi.org/10.1007/s10930-020-09901-4>.
- 441 3. Fernandes, J. D. *et al.* The UCSC SARS-CoV-2 Genome Browser (2020). URL <https://doi.org/10.1038/s41588-020-0697-z>.
- 443 4. Gussow, A. B. *et al.* Genomic determinants of pathogenicity in SARS-CoV-2 and other hu-
444 man coronaviruses. *Proceedings of the National Academy of Sciences* 202008176 (2020).
445 URL <http://www.pnas.org/lookup/doi/10.1073/pnas.2008176117>.
- 446 5. Zhang, Y. Z. & Holmes, E. C. A Genomic Perspective on the Origin and Emer-
447 gence of SARS-CoV-2. *Cell* **181**, 223–227 (2020). URL [/pmc/articles/](#)

- 448 [PMC7194821//pmc/articles/PMC7194821/?report=abstracthttps:](https://pubmed.ncbi.nlm.nih.gov/32811482/)
449 [//www.ncbi.nlm.nih.gov/pmc/articles/PMC7194821/.](https://www.ncbi.nlm.nih.gov/pmc/articles/PMC7194821/)
- 450 6. Kelly, J. A. *et al.* Structural and functional conservation of the programmed 1 ribosomal
451 frameshift signal of SARS coronavirus 2 (SARS-CoV-2). *Journal of Biological Chemistry*
452 **295**, 10741–10748 (2020). URL <http://www.jbc.org/>.
- 453 7. Shean, R. C., Makhsous, N., Stoddard, G. D., Lin, M. J. & Greninger, A. L. VAPiD:
454 A lightweight cross-platform viral annotation pipeline and identification tool to facili-
455 tate virus genome submissions to NCBI GenBank. *BMC Bioinformatics* **20**, 48 (2019).
456 URL [https://bmcbioinformatics.biomedcentral.com/articles/10.](https://bmcbioinformatics.biomedcentral.com/articles/10.1186/s12859-019-2606-y)
457 [1186/s12859-019-2606-y.](https://bmcbioinformatics.biomedcentral.com/articles/10.1186/s12859-019-2606-y)
- 458 8. Seemann, T. Prokka: rapid prokaryotic genome annotation. *Bioinformatics* **30**, 2068–2069
459 (2014). URL [http://www.ncbi.nlm.nih.gov/pubmed/24642063https:](http://www.ncbi.nlm.nih.gov/pubmed/24642063https://academic.oup.com/bioinformatics/article-lookup/doi/10.1093/bioinformatics/btu153)
460 [//academic.oup.com/bioinformatics/article-lookup/doi/10.](https://academic.oup.com/bioinformatics/article-lookup/doi/10.1093/bioinformatics/btu153)
461 [1093/bioinformatics/btu153.](https://academic.oup.com/bioinformatics/article-lookup/doi/10.1093/bioinformatics/btu153)
- 462 9. Jones, P. *et al.* InterProScan 5: genome-scale protein function classification. *Bioin-*
463 *formatics (Oxford, England)* **30**, 1236–40 (2014). URL [http://www.ncbi.nlm.](http://www.ncbi.nlm.nih.gov/pubmed/24451626http://www.pubmedcentral.nih.gov/articlerender.fcgi?artid=PMC3998142)
464 [nih.gov/pubmed/24451626http://www.pubmedcentral.nih.gov/](http://www.ncbi.nlm.nih.gov/pubmed/24451626http://www.pubmedcentral.nih.gov/articlerender.fcgi?artid=PMC3998142)
465 [articlerender.fcgi?artid=PMC3998142.](http://www.ncbi.nlm.nih.gov/pubmed/24451626http://www.pubmedcentral.nih.gov/articlerender.fcgi?artid=PMC3998142)
- 466 10. Koyama, T., Weeraratne, D., Snowdon, J. L. & Parida, L. Emergence of Drift Variants That
467 May Affect COVID-19 Vaccine Development and Antibody Treatment. *Pathogens* **9**, 324
468 (2020).
- 469 11. Chand, M. *et al.* Investigation of novel SARS-CoV-2 variant: Variant of Con-
470 cern 202012/01 Technical Briefing 2. Tech. Rep., Public Health England, Lon-

- 471 don (2020). URL [https://assets.publishing.service.gov.uk/](https://assets.publishing.service.gov.uk/government/uploads/system/uploads/attachment_data/file/949639/Technical_Briefing_VOC202012-2_Briefing_2_FINAL.pdf)
472 [government/uploads/system/uploads/attachment_data/file/](https://assets.publishing.service.gov.uk/government/uploads/system/uploads/attachment_data/file/949639/Technical_Briefing_VOC202012-2_Briefing_2_FINAL.pdf)
473 [949639/Technical_Briefing_VOC202012-2_Briefing_2_FINAL.pdf](https://assets.publishing.service.gov.uk/government/uploads/system/uploads/attachment_data/file/949639/Technical_Briefing_VOC202012-2_Briefing_2_FINAL.pdf).
- 474 12. Report 42 - Transmission of SARS-CoV-2 Lineage B.1.1.7 in England: in-
475 sights from linking epidemiological and genetic data — Faculty of Medicine
476 — Imperial College London. URL [https://www.imperial.ac.](https://www.imperial.ac.uk/mrc-global-infectious-disease-analysis/covid-19/report-42-sars-cov-2-variant/)
477 [uk/mrc-global-infectious-disease-analysis/covid-19/](https://www.imperial.ac.uk/mrc-global-infectious-disease-analysis/covid-19/report-42-sars-cov-2-variant/)
478 [report-42-sars-cov-2-variant/](https://www.imperial.ac.uk/mrc-global-infectious-disease-analysis/covid-19/report-42-sars-cov-2-variant/).
- 479 13. US COVID-19 Cases Caused by Variants — CDC. URL [https://www.cdc.gov/](https://www.cdc.gov/coronavirus/2019-ncov/transmission/variant-cases.html)
480 [coronavirus/2019-ncov/transmission/variant-cases.html](https://www.cdc.gov/coronavirus/2019-ncov/transmission/variant-cases.html).
- 481 14. Hadfield, J. *et al.* Nextstrain: real-time tracking of pathogen evolution. *Bioinformatics*
482 **34**, 4121–4123 (2018). URL [https://academic.oup.com/bioinformatics/](https://academic.oup.com/bioinformatics/article/34/23/4121/5001388)
483 [article/34/23/4121/5001388](https://academic.oup.com/bioinformatics/article/34/23/4121/5001388).
- 484 15. Langmead, B. & Salzberg, S. L. Fast gapped-read alignment with Bowtie 2. *Nature*
485 *methods* **9**, 357–9 (2012). URL [http://www.ncbi.nlm.nih.gov/pubmed/](http://www.ncbi.nlm.nih.gov/pubmed/22388286)
486 [22388286](http://www.ncbi.nlm.nih.gov/pubmed/22388286)[http://www.pubmedcentral.nih.gov/articlerender.fcgi?](http://www.pubmedcentral.nih.gov/articlerender.fcgi?artid=PMC3322381)
487 [artid=PMC3322381](http://www.pubmedcentral.nih.gov/articlerender.fcgi?artid=PMC3322381).
- 488 16. Callaway, E. The coronavirus is mutating - does it matter? (2020).
- 489 17. Neches, R. Y., McGee, M. D. & Kyrpides, N. C. Recombination should not be an af-
490 terthought. *Nature Reviews Microbiology* (2020). URL [http://www.nature.com/](http://www.nature.com/articles/s41579-020-00451-1)
491 [articles/s41579-020-00451-1](http://www.nature.com/articles/s41579-020-00451-1).

- 492 18. Benson, D. A., Karsch-Mizrachi, I., Lipman, D. J., Ostell, J. & Sayers, E. W. GenBank.
493 *Nucleic Acids Research* **37**, D26–D31 (2009). URL [https://academic.oup.com/
494 nar/article-lookup/doi/10.1093/nar/gkn723](https://academic.oup.com/nar/article-lookup/doi/10.1093/nar/gkn723).
- 495 19. Elbe, S. & Buckland-Merrett, G. Data, disease and diplomacy: GISAID’s innova-
496 tive contribution to global health. *Global Challenges* **1**, 33–46 (2017). URL [http:
497 //doi.wiley.com/10.1002/gch2.1018](http://doi.wiley.com/10.1002/gch2.1018).
- 498 20. Seabolt, E. *et al.* IBM Functional Genomics Platform, A Cloud-Based Platform for Study-
499 ing Microbial Life at Scale. *IEEE/ACM Transactions on Computational Biology and Bioin-
500 formatics* 1–1 (2020).
- 501 21. Apweiler, R. *et al.* UniProt: the universal protein knowledgebase. *Nucleic acids research*
502 **45**, D158–D169 (2016).
- 503 22. Hulo, C. *et al.* ViralZone: A knowledge resource to understand virus diversity. *Nu-
504 cleic Acids Research* **39** (2011). URL [https://pubmed.ncbi.nlm.nih.gov/
505 20947564/](https://pubmed.ncbi.nlm.nih.gov/20947564/).
- 506 23. Bauer, D. C. *et al.* Supporting pandemic response using genomics and bioinformatics: A
507 case study on the emergent SARS-CoV-2 outbreak. *Transboundary and Emerging Dis-
508 eases* **67**, 1453–1462 (2020). URL [https://onlinelibrary.wiley.com/doi/
509 10.1111/tbed.13588](https://onlinelibrary.wiley.com/doi/10.1111/tbed.13588).
- 510 24. Lemoine, F., Blassel, L., Voznica, J. & Gascuel, O. COVID-Align: Accurate online
511 alignment of hCoV-19 genomes using a profile HMM (2020). URL [https://www.
512 biorxiv.org/content/10.1101/2020.05.25.114884v1](https://www.biorxiv.org/content/10.1101/2020.05.25.114884v1)[https://www.
513 biorxiv.org/content/10.1101/2020.05.25.114884v1.abstract](https://www.biorxiv.org/content/10.1101/2020.05.25.114884v1.abstract).

- 514 25. Liu, B. *et al.* CoV-Seq, a new tool for SARS-CoV-2 genome analysis and visualization:
515 Development and usability study. *Journal of Medical Internet Research* **22**, e22299 (2020).
516 URL <https://www.jmir.org/2020/10/e22299>.
- 517 26. V'kovski, P., Kratzel, A., Steiner, S., Stalder, H. & Thiel, V. Coronavirus biology and
518 replication: implications for SARS-CoV-2 (2020). URL www.nature.com/nrmicro.
- 519 27. Starr, T. N. *et al.* Deep Mutational Scanning of SARS-CoV-2 Receptor Binding Domain
520 Reveals Constraints on Folding and ACE2 Binding. *Cell* **182**, 1295–1310 (2020).
- 521 28. Yurkovetskiy, L. *et al.* SARS-CoV-2 Spike protein variant D614G increases infectivity
522 and retains sensitivity to antibodies that target the receptor binding domain. *bioRxiv : the*
523 *preprint server for biology* (2020).
- 524 29. Plante, J. A. *et al.* Spike mutation D614G alters SARS-CoV-2 fitness. *Nature* **592**, 116–121
525 (2021).
- 526 30. Xie, X. *et al.* Neutralization of SARS-CoV-2 spike 69/70 deletion, E484K and N501Y
527 variants by BNT162b2 vaccine-elicited sera. *Nature Medicine* **27**, 620–621 (2021). URL
528 <https://doi.org/10.1038/s41591-021-01270-4>.
- 529 31. Kupferschmidt, K. Fast-spreading U.K. virus variant raises alarms. *Science* **371**, 9–10
530 (2021). URL <http://science.sciencemag.org/content/371/6524/9>.
- 531 32. Altschul, S. F., Gish, W., Miller, W., Myers, E. W. & Lipman, D. J. Basic local alignment
532 search tool. *Journal of Molecular Biology* **215**, 403–410 (1990). URL <https://www.sciencedirect.com/science/article/pii/S0022283605803602>.
533
- 534 33. Pearson, W. R. Selecting the right similarity-scoring matrix. *Current Protocols*
535 *in Bioinformatics* **43**, 3.5.1 (2013). URL [/pmc/articles/PMC3848038/](https://pubmed.ncbi.nlm.nih.gov/23405000/)

536 ?report=abstract<https://www.ncbi.nlm.nih.gov/pmc/articles/>
537 PMC3848038/.

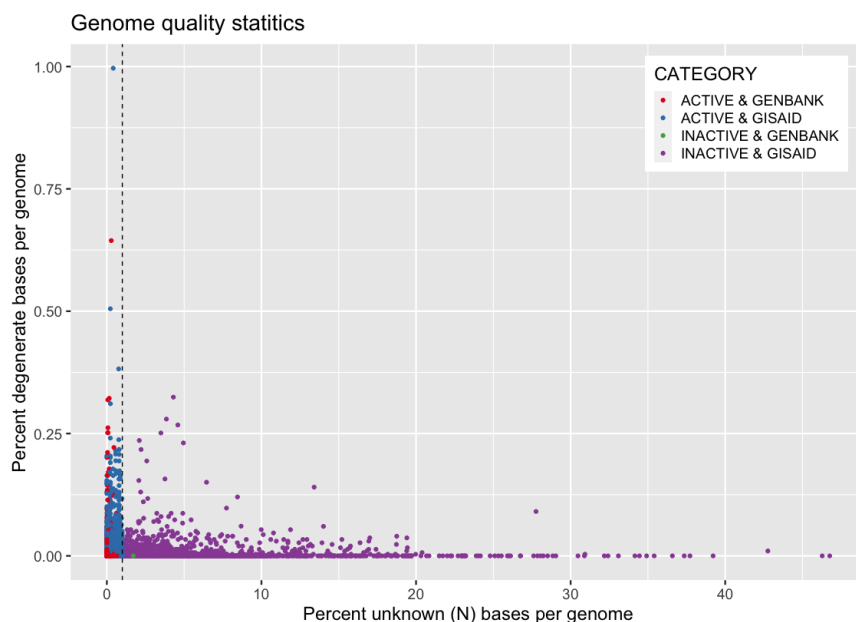
538 **Acknowledgments**

539 We would like to acknowledge the immense collaborative effort from the IBM COVID-19 Task
540 Force to help us open this platform to support research globally for the SARS-CoV-2 pandemic.
541 Additionally, we gratefully acknowledge all the authors from the originating laboratories re-
542 sponsible for obtaining the specimens and the submitting laboratories where SARS-CoV-2 ge-
543 netic sequence data were generated and shared via the GISAID Initiative, on which part of this
544 research is based.

545 **Supplementary materials**

- 546 • Supplementary File 1: SARS-CoV-2 Genome Acknowledgements (txt)
- 547 • Supplementary File 2: Non-redundant Protein Sequences (fasta.gz)
- 548 • Supplementary File 3: Genome and Protein Mapping Information (csv)
- 549 • Supplementary File 4: Spike Glycoprotein Domain Named Sequences (csv)
- 550 • Supplementary File 5: Protein and Domain Mapping Information (tsv)

(a)



(b)

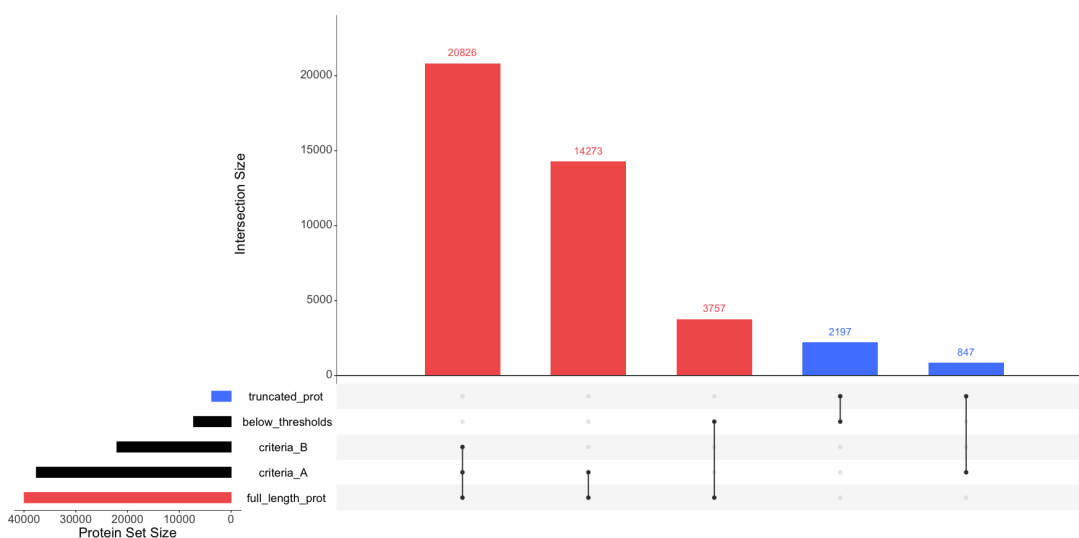


Figure 1: SARS-CoV-2 genome quality observations and their effect on annotation results. The percent of unknown (N) and degenerate bases (as defined by IUPAC) are calculated as a function of total genome size for SARS-COV-2 genomes from two sources: NCBI GenBank and GISAID (**1a**). The quality threshold of unknown bases is indicated with a dashed line. Also, full length (red) or truncated (blue) protein products are indicated for genomes by quality criteria status: our selected criteria (Criteria A), a more stringent criteria (Criteria B), or below quality thresholds (**1b**). For criteria definitions, see Section 4.1.

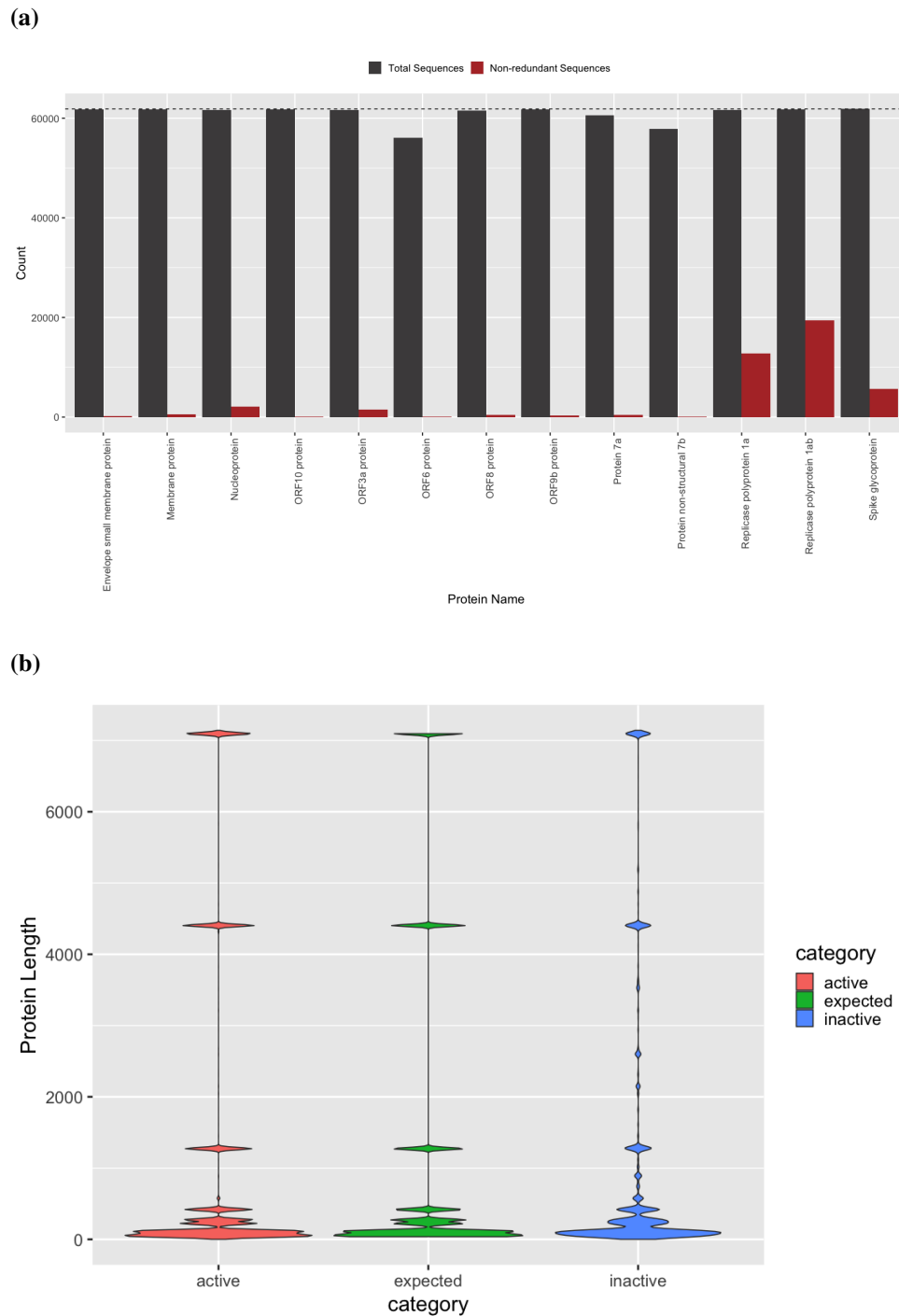


Figure 2: **Protein annotation set membership and sequence accuracy.** Set membership of all (grey) and distinct (red) protein sequences identified in SARS-CoV-2 genomes above quality thresholds (**2a**). Count indicates the number of times a given protein was observed in the entire active genome corpus (dashed line). (**2b**) Protein size distribution of known protein references (expected, green) more closely matches our *in silico* predicted protein sequences from genomes above quality thresholds (active genomes, red) compared to products predicted from genomes below quality thresholds (inactive genomes, blue).

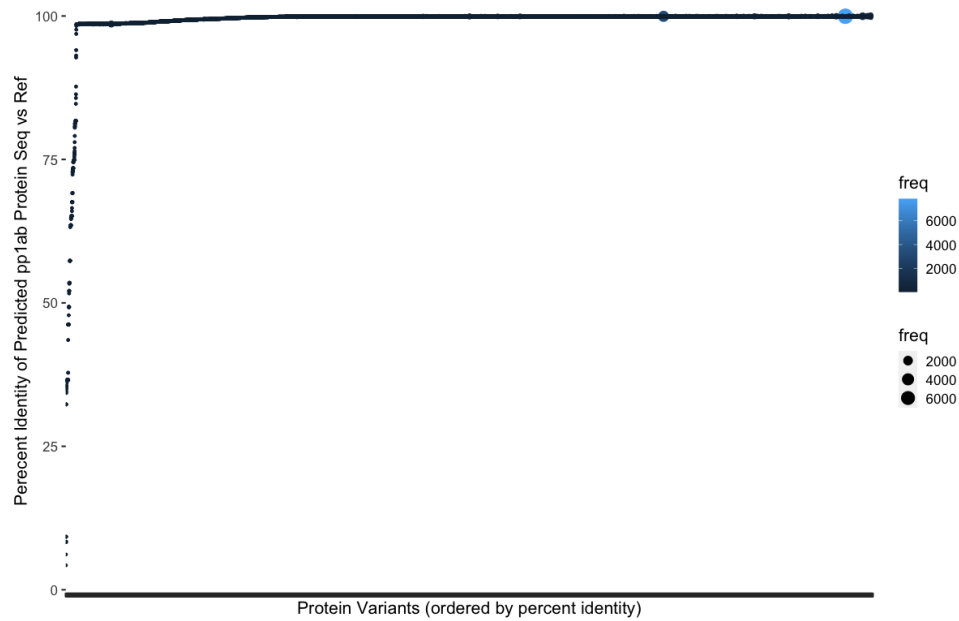


Figure 3: For Replicase polyprotein 1ab, the variant frequency and sequence similarity of our predicted protein to the known UniProt ID:P0DTD1 references is shown

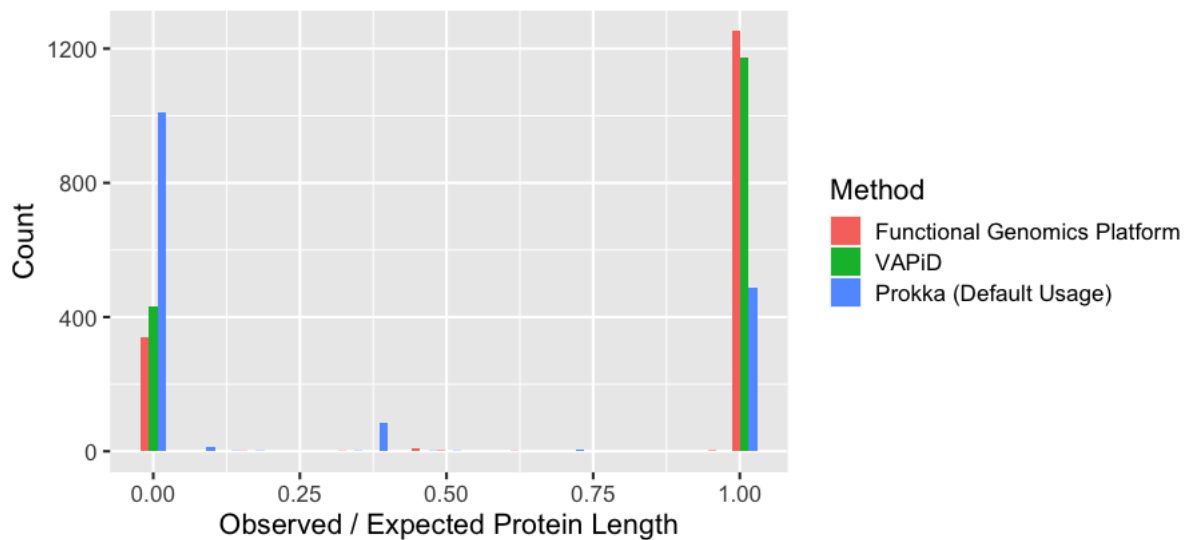
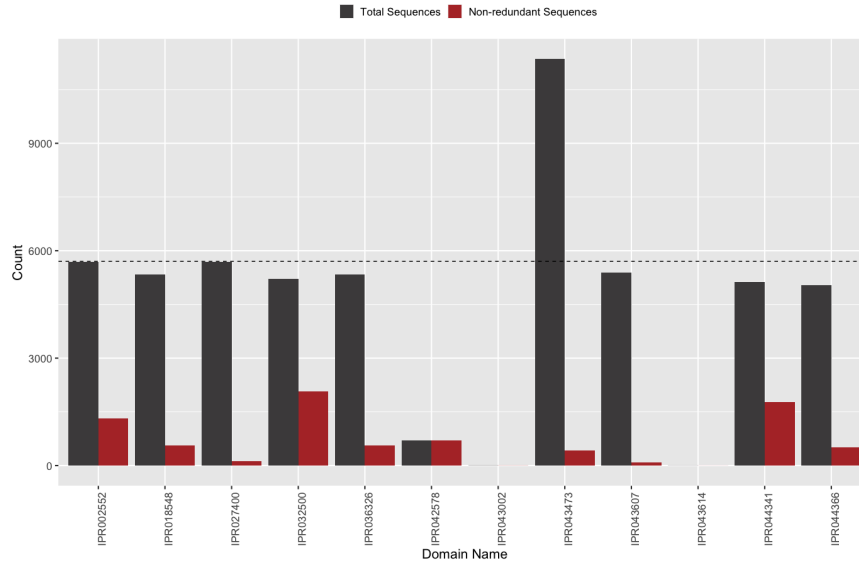


Figure 4: Protein length comparisons against known reference sequences for three pipelines: Functional Genomics Platform (our method), VAPiD, Prokka with default usage for viral genomes. The count of protein sequences at each observed / expected value is plotted for each pipeline. Length is set to zero if a protein is missing in the results from that pipeline but present in another.

(a)



(b)

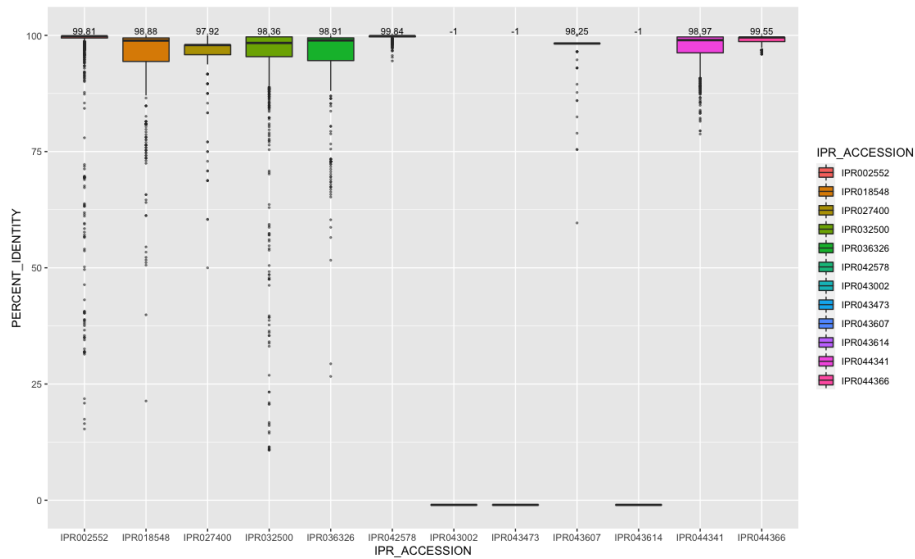
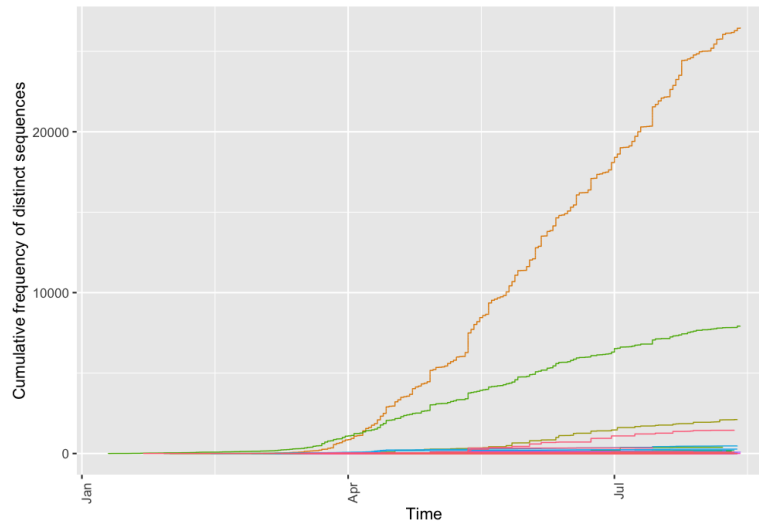


Figure 5: **Domain annotation set membership and sequence accuracy for spike glycoprotein.** Set membership of all (grey) and distinct (red) domain sequences identified in spike glycoprotein (5a). Count indicates the number of times a given domain was observed for all S proteins (dashed line). (5b) indicates the percent identity of our predicted domain sequences against reference domain sequences where possible to be calculated. In the absence of a reference sequence, percent identity is indicated as -1.

(a)



(b)

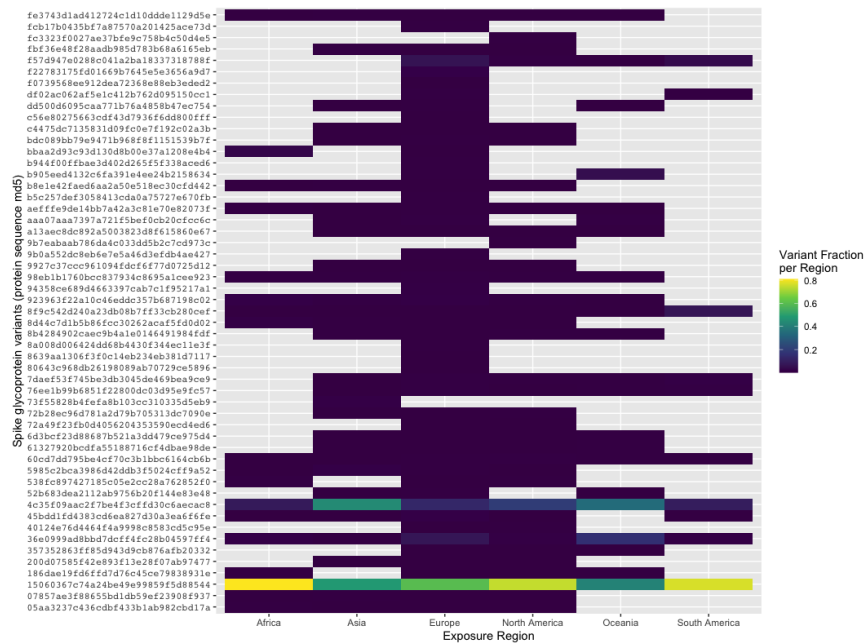


Figure 6: Spike glycoprotein variants observed in SARS-CoV-2 genomes over time and geography. Each line represents the cumulative frequency per variant (orange: D614G, green: UniProt ID P0DTC2, olive: P1140X, pink: S2 cleavage product) in **6a**. Low frequency S protein sequences (<5 observations) are removed from plotting for simplicity. In **6b**, the proportion of spike glycoprotein variants differ by exposure region. Proportion is calculated per variant to allow inter-region comparisons.